Hanbury Brown and Twiss interferometry of single phonons from an optomechanical resonator

Hong, Sungkun; Riedinger, Ralf; Marinkovic, Igor; Wallucks, Andreas; Hofer, Sebastian G.; Norte, Richard A.; Aspelmeyer, Markus; Groeblacher, Simon

DOI
10.1126/science.aan7939

Publication date
2017

Document Version
Final published version

Published in
Science

QUANTUM SYSTEMS

Hanbury Brown and Twiss interferometry of single phonons from an optomechanical resonator

Sungkun Hong,[1]* Ralf Riedinger,[1]* Igor Marinković,[2]* Andreas Wallucks,[2]* Sebastian G. Hofer,[1] Richard A. Norte,[2] Markus Aspelmeyer,[1]† Simon Gröblacher[2]†

Nano- and micromechanical solid-state quantum devices have become a focus of attention. Reliably generating nonclassical states of their motion is of interest both for addressing fundamental questions about macroscopic quantum phenomena and for developing quantum technologies in the domains of sensing and transduction. We used quantum optical control techniques to conditionally generate single-phonon Fock states of a nanomechanical resonator. We performed a Hanbury Brown and Twiss–type experiment that verified the nonclassical nature of the phonon state without requiring full state reconstruction. Our result establishes purely optical quantum control of a mechanical oscillator at the single-phonon level.

Intensity correlations in electromagnetic fields have been pivotal in the development of modern quantum optics. The experiments by Hanbury Brown and Twiss were a particular milestone that connected the temporal and spatial coherence properties of a light source with the second-order intensity autocorrelation function $g^{(2)}(\tau, x)$ (*1*–*3*). In essence, $g^{(2)}$ correlates intensities measured at times differing by τ or at locations differing by x and hence is a measure of their joint detection probability. At the same time, these correlations allow the quantum nature of the underlying field to be inferred directly. For example, a classical light source of finite coherence time can only exhibit positive correlations at a delay of $\tau \approx 0$ in the joint intensity detection probability, leading to bunching in the photon arrival time. This result holds true for all bosonic fields. Fermions, on the other hand, exhibit negative correlations and hence antibunching in the detection events (*4*–*6*), which is a manifestation of the Pauli exclusion principle. A bosonic system needs to be in a genuine nonclassical state to exhibit antibunching. The canonical example is a single-photon (Fock) state, for which $g^{(2)}(\tau = 0) = 0$ because no joint detection can take place (*7*). For this reason, measuring $g^{(2)}$ has become a standard method to characterize the purity of single-photon sources (*8*). In general, $g^{(2)}(\tau)$ carries a wealth of information on the statistical properties of a bosonic field with no classical analog (*9*, *10*)—specifically, sub-Poissonian counting statistics [$g^{(2)}(0) < 1$] and antibunching [$g^{(2)}(\tau) \geq g^{(2)}(0)$]—all of which have been demonstrated successfully with quantum states of light (*11*, *12*).

Over the past decade, motional degrees of freedom (phonons) of solid-state devices have emerged as a quantum resource. Quantum control of phonons was pioneered in the field of trapped ions (*13*), where single excitations of the motion of the ions are manipulated through laser light. These single-phonon states have been used for fundamental studies of decoherence (*14*) and for elementary transduction channels in quantum gates for universal quantum computing (*15*). Cavity optomechanics (*16*) has successfully extended these ideas to optically controlling the collective motion of solid-state mechanical systems. It has allowed for remarkable progress in controlling solid-state phonons at the quantum level, including sideband cooling into the quantum ground state of motion (*17*, *18*), the generation of quantum correlated states between radiation fields and mechanical motion (*19*–*21*), and the generation of squeezed motional states (*22*–*24*).

So far, single-phonon manipulation of micromechanical systems has exclusively been achieved through coupling to superconducting qubits (*25*–*27*), and optical control has been limited to the generation of quantum states of bipartite systems (*20*, *21*, *28*). Here we demonstrate all-optical quantum control of a purely mechanical system, creating phonons at the single-quantum level and unambiguously showing their nonclassical nature. We combined optomechanical control of motion and single-phonon counting techniques (*21*, *29*) to probabilistically generate a single-phonon Fock state from a nanomechanical device. Implementing Hanbury Brown and Twiss interferometry for phonons (*21*, *29*) (Fig. 1) allowed us to probe the quantum mechanical character of single phonons without reconstructing their states. We observed $g^{(2)}(0) < 1$, which is a direct verification of the nonclassicality of the optomechanically generated phonons, highlighting their particle-like behavior.

Our optomechanical crystal (*18*) consists of a microfabricated silicon nanobeam patterned so that it simultaneously acts as a photonic and phononic resonator (Fig. 2). The resulting optical and mechanical modes couple through radiation pressure and the photoelastic effect so that a displacement equivalent to the zero-point fluctuation of the mechanical mode leads to a frequency shift of the optical mode by $g_0/2\pi = 869$ kHz (g_0, optomechanical coupling rate). The optical resonance has a wavelength $\lambda = 1554.35$ nm and a critically coupled total quality factor $Q_o = 2.28 \times 10^5$ (cavity energy decay rate $\kappa/2\pi = 846$ MHz), whereas the mechanical resonance has a frequency of $\omega_m/2\pi = 5.25$ GHz and a quality factor of $Q_m = 3.8 \times 10^5$. The device is placed in a dilution refrigerator with a base temperature of $T = 35$ mK. When the device is thermalized, its high frequency guarantees that the mechanical mode is initialized deep in its quantum ground state (*21*).

We utilized two types of linearized optomechanical interactions—the parametric down-conversion and the state swap—which can be realized by driving the system with detuned laser beams in the limit of weak coupling ($g_0\sqrt{n_c} \ll \kappa$, where n_c is the intracavity photon number) and resolved sidebands ($\kappa \ll \omega_m$) (*16*). The parametric down-conversion interaction has the form $H_{dc} = \hbar g_0 \sqrt{n_c}(\hat{a}^\dagger \hat{b}^\dagger + \hat{a}\hat{b})$, where $\hbar$ is the reduced Planck constant; $\hat{b}^\dagger$ and $\hat{b}$ are the phononic creation and annihilation operators, respectively; and $\hat{a}^\dagger$ and $\hat{a}$ are the respective photonic operators. This interaction is selectively turned on by detuning the laser frequency ω_L to the blue side of the cavity resonance ω_c ($\omega_L = \omega_c + \omega_m$). H_{dc} drives the joint optical and mechanical state, initially in the ground state, into the state $|\psi\rangle_{om} \propto |00\rangle + p_b^{1/2}|11\rangle + p_b|22\rangle + O(p_b^{3/2})$. For low excitation probabilities $p_b \ll 1$, higher-order terms can be neglected so that the system can be approximated as emitting a pair consisting of a resonant signal photon and an idler phonon with a probability p_b (*30*). Detection of the signal photon emanating from the device heralds a single excitation of the mechanical oscillator $|\psi\rangle_m \approx |1\rangle$, in close analogy to heralded single photons from spontaneous parametric down-conversion. To read out the phonon state, we send in another laser pulse that is now red-detuned from the cavity resonance by ω_m ($\omega_L = \omega_c - \omega_m$). This realizes a state-swap interaction $H_{swap} = \hbar g_0 \sqrt{n_c}(\hat{a}^\dagger \hat{b} + \hat{a}\hat{b}^\dagger)$, which transfers the mechanical state to the optical mode with efficiency p_r. We can therefore use the scattered light field from this "read" operation to directly measure the second-order intensity correlation function $g^{(2)}$ of the mechanical oscillator mode, which is defined as

$$g^{(2)}(\tau) = \frac{\left\langle \hat{b}^\dagger(0)\hat{b}^\dagger(\tau)\hat{b}(\tau)\hat{b}(0)\right\rangle}{\left\langle \hat{b}^\dagger(0)\hat{b}(0)\right\rangle \left\langle \hat{b}^\dagger(\tau)\hat{b}(\tau)\right\rangle} \quad (1)$$

where τ is the time between the first and the second detection event. Like for any other bosonic system, $g^{(2)}(0) > 1$ means that the phonons exhibit super-Poissonian (classical) behavior, whereas $g^{(2)}(0) < 1$ is direct evidence of the quantum mechanical nature of the state and implies sub-Poissonian phonon statistics (*10*).

We implemented the experimental approach (Fig. 1) by repeatedly sending a pair of optical

[1]Vienna Center for Quantum Science and Technology, Faculty of Physics, University of Vienna, A-1090 Vienna, Austria. [2]Kavli Institute of Nanoscience, Delft University of Technology, 2628CJ Delft, Netherlands.
*These authors contributed equally to this work. †Corresponding author. Email: markus.aspelmeyer@univie.ac.at (M.A.); s.groeblacher@tudelft.nl (S.G.)

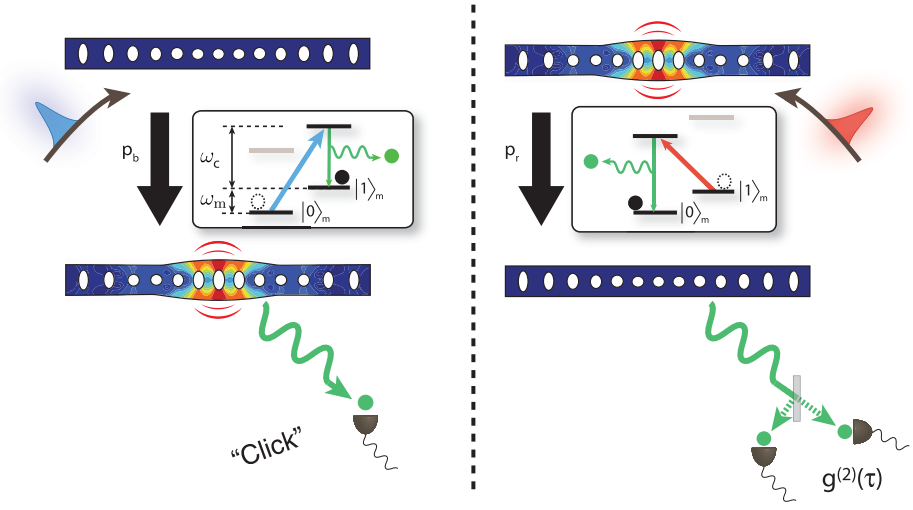

Fig. 1. Working principle of the approach used to generate single-phonon states and verify their nonclassicality. The first step (**left**) starts with a mechanical oscillator in its quantum ground state, followed by pumping the optomechanical cavity with a blue-detuned pulse. The resonator is excited to a single-phonon state with a probability p_b = 1.2% through the optomechanical interaction, which is accompanied by the emission of a photon on resonance with the cavity. The detection of such a photon in a single-photon detector (indicated by the "click") allows us to post-select on a purely mechanical Fock state. To verify the quantum state that we created, a red-detuned read pulse is sent onto the optomechanical cavity in the second step (**right**), which performs a partial state transfer between the optics and the mechanics. With a probability of p_r = 32.5%, the mechanical system's excitation is converted into a photon on cavity resonance, returning the mechanics to its ground state. The photon is sent onto a beamsplitter, where we measure the second-order intensity correlation function $g^{(2)}$ by using a pair of single-photon detectors. $g^{(2)}(0) < 1$ confirms the nonclassicality of the generated phonon states. The insets show the equivalent energy level diagrams of the processes.

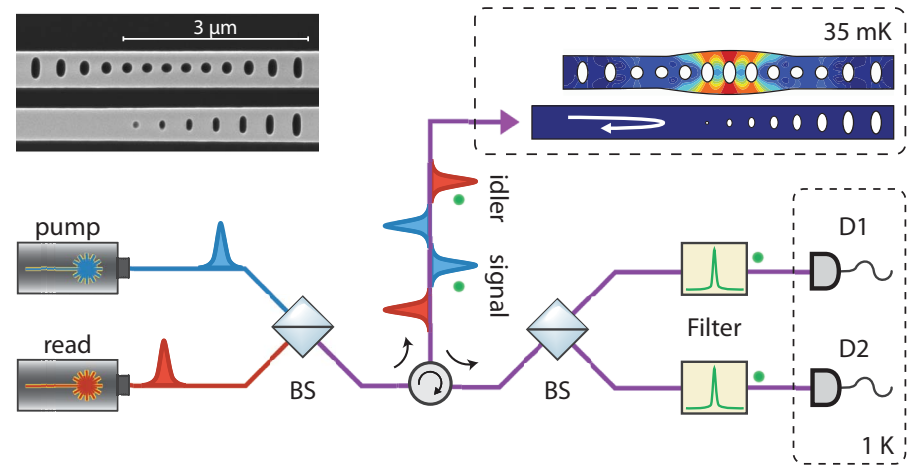

Fig. 2. Sketch of the experimental setup used to measure the intensity autocorrelation function $g^{(2)}$ of phonons. Blue-detuned pump pulses are sent into the optomechanical cavity, which is kept at 35 mK. With a small probability p_b, the optomechanical interaction creates a single excitation of the mechanical mode at 5.25 GHz (idler) and at the same time emits a signal photon on resonance with the cavity. The original optical pump field is then filtered, and only the signal photon created in the optomechanical down-conversion process is detected in one of the single-photon detectors (D1 or D2). With a time delay t_d, a red-detuned read pulse is sent into the device, converting any mechanical idler excitation into an idler photon, which again is filtered from the original pump. Conditioned on the detection of a signal photon, we measure the $g^{(2)}$ of the idler photons. Because the red-detuned pulse is equivalent to a state-swap interaction, the $g^{(2)}$ function that we obtain for the photons is a direct measure of the $g^{(2)}$ function of the phonons in the mechanical oscillator. The inset in the top left corner shows a scanning electron microscope image of the device (top) next to a waveguide (bottom). BS, beamsplitter.

pulses, the first one blue-detuned [pump pulse, full width at half maximum (FWHM) ≈ 32 ns] and the second one red-detuned (read pulse, FWHM ≈ 32 ns), with a fixed repetition period T_r = 50 μs. Photons generated through the optomechanical interactions were reflected back from the device and analyzed by a Hanbury Brown and Twiss interferometer using two superconducting nanowire single-photon detectors (SNSPDs). We set the mean pump pulse energy to 27 fJ so that p_b = 1.2% (*31*). Detection of resonant (signal) photons created by this pulse heralds the preparation of the mechanical oscillator in a single-phonon Fock state, in principle with a probability of 98.8%. Owing to a small amount of initial thermal phonons and residual absorption heating, a fraction of unwanted phonons were incoherently added to the quantum states that we prepared (*21*). After each pump pulse, a red-detuned read pulse was sent to the device with a programmable delay t_d, reading out phonons stored in the device by converting them into photons on resonance with the cavity. The mean read pulse energy was set to 924 fJ, corresponding to a state-swap efficiency p_r ≈ 32.5%. Taking into account subsequent optical scattering losses, this yields an absolute quantum efficiency for the detection of phonons of 0.9% (*31*). Last, the pulse repetition period of T_r = 50 μs, which is long compared with the mechanical damping time of 11 μs, provides ample time for dissipating any excitation or unwanted heating generated by optical absorption. This ensured that each experimental cycle started with the mechanical mode well in the quantum ground state. The pulse sequence was repeated more than 7×10^9 times to acquire enough statistics. Conditioned on heralding events from detector D1 by the blue-detuned pulses, we analyzed the coincidence detection probability of photons at D1 and D2 that are transferred from phonons by the swap operation.

In our first experiment, we set t_d = 115 ns and measured $g^{(2)}(0)$ of the heralded phonons. One of our SNSPDs, D2, exhibited a longer dead time than t_d (*31*), and we therefore only used photon counts from D1 for heralding the phonon states. From these measurements, we obtained a $g^{(2)}(0)$ of $0.65^{+0.11}_{-0.08}$ (Fig. 3C), demonstrating a nonclassical character of the mechanical state.

The observed $g^{(2)}(0)$ of 0.65 is considerably higher than what we expect in the ideal case, $g^{(2)}_{ideal}(0) \approx 4 \times p_b = 0.045$ (*31*). We attribute this to heating induced by the absorption of the pump and read pulses. Although a detailed physical mechanism for the absorption and subsequent heat transfer into the mechanical mode is still a subject of study (*21*), the influx of thermal phonons $\dot{n}_{abs}$ caused by the absorption of drive laser pulses can be experimentally deduced from the (unconditional) photon count rates generated by the read pulses (*31*). Including an estimation of the initial thermal phonon number n_{init}, which is likewise inferred from the unconditional photon counts associated with the pump and read pulses, we constructed a theoretical model that predicts $g^{(2)}(0)$ as a function of p_b, n_{init}, and $\dot{n}_{abs}$. Given the measured $n_{init} \approx 0.20$ and $\dot{n}_{abs}$ (*31*)

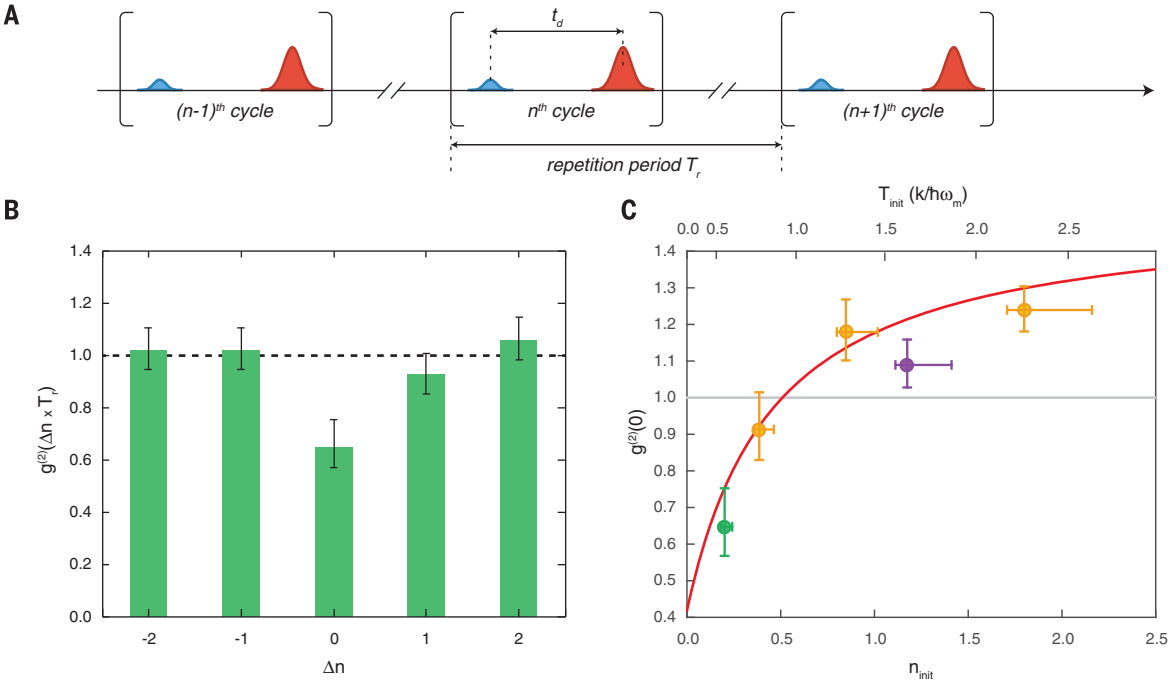

Fig. 3. Experimental single-phonon creation and Hanbury Brown and Twiss interferometry. (**A**) Pulse sequence used in the experiments. Each cycle consists of a blue-detuned pump pulse and a subsequent red-detuned read pulse delayed by t_d. The pulse sequence is repeated with the period T_r. Both t_d and T_r can be adjusted. (**B**) The measurement result of the second-order correlation function $g^{(2)}(\tau = \Delta n \times T_r)$ of the heralded phonons, with $g^{(2)}(0) < 1$ being a direct measure of their nonclassicality. In this measurement, we set t_d = 115 ns and T_r = 50 μs. $g^{(2)}(\Delta n \times T_r)$ with $\Delta n \neq 0$ depicts the correlations between phonons read from separate pulse sequences with the cycle difference of Δn. Whereas phonons from independent pulses show no correlation [$g^{(2)}(\Delta n \times T_r; \Delta n \neq 0) \approx 1$], those from the same read pulse are strongly anticorrelated $\left[g^{(2)}(\tau = 0) = 0.65^{+0.11}_{-0.08}\right]$. (**C**) The influence of an incoherent phonon background on the $g^{(2)}(0)$ of the generated mechanical states. Several measurements are plotted for a range of different effective initial temperatures of the nanomechanical oscillator. The first data point (green) was taken with a delay t_d = 115 ns and a repetition period T_r = 50 μs. We control the initial mode occupation n_{init} (initial mode temperature T_{init}) by using the long lifetime of the thermally excited phonons stemming from the delayed absorption heating by pump and read pulses. This allows us to increase n_{init} while keeping the bulk temperature and properties of the device constant, causing an increase in $g^{(2)}(0)$ as the state becomes more thermal. The red line shows the simulated $g^{(2)}(0)$ as discussed in (*31*). For technical reasons, all data points (yellow and purple) except the leftmost (green) were taken with t_d = 95 ns. In addition, the second from the right (purple) was taken at an elevated bath temperature of T_{bath} = 160 mK.

within the read pulse, our model predicts $g^{(2)}(0) \approx 0.76$, which is consistent with the experimental value.

To further probe the effect of thermal phonons, we performed a set of experiments with reduced repetition periods T_r, while keeping the other settings for the pump pulses the same. This effectively increases n_{init}, because the absorbed heat does not have enough time to dissipate before the next pair of pulses arrives. As expected, as T_r was reduced, we observed an increase in $g^{(2)}(0)$. With the measured n_{init} and $\dot{n}_{abs}$ from the same data set, we can plot the predicted $g^{(2)}(0)$ values. The experimental values and theoretical bounds on $g^{(2)}(0)$ are in good agreement (Fig. 3).

We also measured $g^{(2)}(0)$ for t_d = 350 ns and found that it increased to $0.84^{+0.07}_{-0.06}$. This increase is consistent with previously observed delayed heating effects of the absorption (*21*) and is in good agreement with the theoretical prediction of 0.84. Even for these longer delays, the value is still below 1, demonstrating the potential of our device as a single-phonon quantum memory on the time scale of several hundred nanoseconds.

We experimentally demonstrated the quantum nature of heralded single phonons in a nanomechanical oscillator by measuring their intensity correlation function $g^{(2)}(0) < 1$. The deviation from a perfect single-phonon state can be modeled by a finite initial thermal occupation and additional heating from our optical cavity fields. We achieved conversion efficiencies between phonons and telecom photons of more than 30%, only limited by our available laser power and residual absorption. Full state reconstruction of the single-phonon state, as demonstrated with phononic states of trapped ions (*14*), should be realizable with slightly improved readout efficiency and through homodyne tomography. The demonstrated fully optical quantum control of a nanomechanical mode, preparing sub-Poissonian phonons, shows that optomechanical cavities are a useful resource for future integrated quantum phononic devices, as both single-phonon sources and detectors. They are also an ideal candidate for storage of quantum information in mechanical excitations and constitute a fundamental building block for quantum information processing involving phonons. Some of the potential applications include quantum noise–limited, coherent microwave-to-optics conversion, as well as studying the quantum behavior of individual phonons of a massive system.

REFERENCES AND NOTES

1. R. Hanbury Brown, R. Q. Twiss, *Nature* **177**, 27–29 (1956).
2. R. Hanbury Brown, R. Q. Twiss, *Nature* **178**, 1046–1048 (1956).
3. B. L. Morgan, L. Mandel, *Phys. Rev. Lett.* **16**, 1012–1015 (1966).
4. M. Henny *et al.*, *Science* **284**, 296–298 (1999).
5. W. D. Oliver, J. Kim, R. C. Liu, Y. Yamamoto, *Science* **284**, 299–301 (1999).
6. T. Jeltes *et al.*, *Nature* **445**, 402–405 (2007).
7. P. Grangier, G. Roger, A. Aspect, *Europhys. Lett.* **1**, 173–179 (1986).
8. M. D. Eisaman, J. Fan, A. Migdall, S. V. Polyakov, *Rev. Sci. Instrum.* **82**, 071101 (2011).
9. X. T. Zou, L. Mandel, *Phys. Rev. A* **41**, 475–476 (1990).
10. L. Davidovich, *Rev. Mod. Phys.* **68**, 127–173 (1996).
11. H. J. Kimble, M. Dagenais, L. Mandel, *Phys. Rev. Lett.* **39**, 691–695 (1977).
12. R. Short, L. Mandel, *Phys. Rev. Lett.* **51**, 384–387 (1983).
13. R. Blatt, D. Wineland, *Nature* **453**, 1008–1015 (2008).
14. D. Leibfried *et al.*, *Phys. Rev. Lett.* **77**, 4281–4285 (1996).
15. J. I. Cirac, P. Zoller, *Phys. Rev. Lett.* **74**, 4091–4094 (1995).
16. M. Aspelmeyer, T. J. Kippenberg, F. Marquardt, *Rev. Mod. Phys.* **86**, 1391–1452 (2014).
17. J. D. Teufel *et al.*, *Nature* **475**, 359–363 (2011).
18. J. Chan *et al.*, *Nature* **478**, 89–92 (2011).
19. T. A. Palomaki, J. D. Teufel, R. W. Simmonds, K. W. Lehnert, *Science* **342**, 710–713 (2013).
20. K. C. Lee *et al.*, *Science* **334**, 1253–1256 (2011).
21. R. Riedinger *et al.*, *Nature* **530**, 313–316 (2016).
22. E. E. Wollman *et al.*, *Science* **349**, 952–955 (2015).
23. J.-M. Pirkkalainen, E. Damskägg, M. Brandt, F. Massel, M. A. Sillanpää, *Phys. Rev. Lett.* **115**, 243601 (2015).
24. F. Lecocq, J. B. Clark, R. W. Simmonds, J. Aumentado, J. D. Teufel, *Phys. Rev. X* **5**, 041037 (2015).
25. A. D. O'Connell *et al.*, *Nature* **464**, 697–703 (2010).
26. Y. Chu *et al.*, *Science* **358**, 199–202 (2017).

27. A. P. Reed *et al*., *Nat. Phys.* 10.1038/nphys4251 (2017).
28. K. C. Lee *et al*., *Nat. Photonics* **6**, 41–44 (2012).
29. J. D. Cohen *et al*., *Nature* **520**, 522–525 (2015).
30. S. G. Hofer, W. Wieczorek, M. Aspelmeyer, K. Hammerer, *Phys. Rev. A* **84**, 052327 (2011).
31. See the supplementary materials.

ACKNOWLEDGMENTS

We thank V. Anant, J. Hofer, C. Loeschnauer, R. Patel, and A. Safavi-Naeini for experimental support and K. Hammerer for helpful discussions. We acknowledge assistance from the Kavli Nanolab Delft, in particular from M. Zuiddam and C. de Boer. This project was supported by the European Commission under the Marie Curie Horizon 2020 initial training programme OMT (grant 722923); the Foundation for Fundamental Research on Matter (FOM) Projectruimte (grants 15PR3210 and 16PR1054;) the Vienna Science and Technology Fund (WWTF; grant ICT12-049); the European Research Council (Consolidator Grant QLev4G and Starting Grant Strong-Q); the Austrian Science Fund (FWF) under projects F40 (SFB FOQUS) and P28172; and the Netherlands Organisation for Scientific Research (NWO/OCW) as part of the Frontiers of Nanoscience program, as well as through a Vidi grant (016.159.369). R.R. is supported by the FWF under project W1210 (CoQuS) and is a recipient of a DOC fellowship of the Austrian Academy of Sciences at the University of Vienna. All relevant data to understand and assess the conclusions of this research are available in the main text and supplementary materials.

SUPPLEMENTARY MATERIALS

www.sciencemag.org/content/358/6360/203/suppl/DC1
Materials and Methods
Figs. S1 to S3
References (*32*–*48*)

24 May 2017; accepted 30 August 2017
Published online 21 September 2017
10.1126/science.aan7939

Hanbury Brown and Twiss interferometry of single phonons from an optomechanical resonator

Sungkun Hong, Ralf Riedinger, Igor Marinkovic, Andreas Wallucks, Sebastian G. Hofer, Richard A. Norte, Markus Aspelmeyer and Simon Gröblacher

Science **358** (6360), 203-206.
DOI: 10.1126/science.aan7939originally published online September 21, 2017

Mechanical systems at the quantum level

A number of platforms are being pursued for developing technologies that exploit the enhanced sensing and measurement capabilities of quantum mechanics. Hybrid systems offer the flexibility of combining and optimizing different platforms. Hong *et al.* combined optomechanical control of motion and single-phonon counting techniques to probabilistically generate a single-phonon Fock state within a nanomechanical resonator. Chu *et al.* used electromechanical coupling to address a bulk piezoelectric resonator with a superconducting quantum circuit. Both approaches hold promise for developing hybrid quantum technologies.

Science, this issue p. 203, p. 199

Science (print ISSN 0036-8075; online ISSN 1095-9203) is published by the American Association for the Advancement of Science, 1200 New York Avenue NW, Washington, DC 20005. The title *Science* is a registered trademark of AAAS.